

**Dynamic scaling for the isotropic ferromagnet:  
 $\epsilon$  expansion to two-loop order\***

Jayanta K. Bhattacharjee and Richard A. Ferrell

*Institute for Science and Technology and Center for Theoretical Physics,  
 Department of Physics and Astronomy, University of Maryland, College Park, Maryland 20742*

(Received 24 April 1981)

The fluctuation spectrum for an isotropic ferromagnet at  $T = T_c$  to  $O(\epsilon)$  is studied by a direct application of the equations of motion. The amplitude of the momentum-dependent relaxation rate is obtained to two-loop order and compared with experimental results.

**I. INTRODUCTION**

The critical dynamics of isotropic ferromagnets,<sup>1-3</sup> although conceptually quite straightforward, have proved to be mathematically somewhat intractable. The calculations of spectral shape have been restricted to single-loop order, and even at this order the fluctuation spectrum does not lend itself to analytic evaluation in the  $\epsilon$  expansion. At  $T = T_c$ , the self-consistent calculation has been performed by Wegner<sup>4</sup> on a computer. The  $\epsilon$  expansion was studied by Dohm<sup>2</sup> using the field theoretic-renormalization group, and later by Nolan and Mazenko<sup>3</sup> with strikingly different answers. While Dohm<sup>2</sup> obtained a spectrum that qualitatively resembled Wegner's<sup>4</sup> self-consistent calculations, Nolan and Mazenko<sup>3</sup> found well-defined structure in the spectrum at  $T_c$ , similar to that predicted for antiferromagnets<sup>5</sup> and liquid helium.<sup>6</sup>

In this paper we study the fluctuation spectrum and the amplitude of the relaxation rate at  $T = T_c$  by  $\epsilon$ -expansion techniques. A subsequent paper will deal with the analytic study of the self-consistent method at  $D = 3$ . There the scaling function for  $T > T_c$  will also be investigated. Our  $\epsilon$  expansion is not based on the renormalization group, but on a direct perturbative solution of the equations of motion.<sup>7</sup> This provides an independent check on the work of Dohm<sup>2</sup> and of Nolan and Mazenko<sup>3</sup> and should help settle the controversy regarding the structure in the spectrum. This equation can be settled by calculating the zero-frequency curvature. It is possible to do this analytically. As shown in Secs. II and III, our answer agrees with that of Dohm<sup>2</sup> (apart from one minor detail) and supports his conclusion regarding

the lack of structure in the spectrum in a first-order  $\epsilon$  expansion. However, our spectrum differs somewhat from the form of Dohm's<sup>2</sup> spectrum because of the different exponentiation. For very high frequencies, the self-energy has a definite scaling form which is not given correctly in a strict  $\epsilon$  expansion. Taking this correct high-frequency behavior into account gives us a spectrum with a tail that dies out more rapidly than found by Dohm.

We have also carried out a two-loop  $\epsilon$ -expansion calculation of the universal amplitude that fixes the frequency scale. Thus we can predict both the shape and scale of the spectrum. The two-loop amplitude is compared with the amplitude for EuO and Co, as measured by Dietrich *et al.*<sup>8</sup> and Glinka *et al.*,<sup>9</sup> respectively. This is done in Sec. III, while Sec. IV provides a brief summary.

**II. FLUCTUATION SPECTRUM**

The order parameter  $\psi$  for the ferromagnet is the magnetization vector with components  $\psi_1, \psi_2,$  and  $\psi_3$ . The equation of motion is the Landau-Lifshitz equation

$$\frac{\partial \vec{\psi}}{\partial t} = g \vec{\psi} \times \nabla^2 \vec{\psi}, \tag{2.1}$$

where  $g$  is some coupling constant. It is convenient to write this equation in momentum space as

$$\dot{\psi}_1(\vec{p}_1) = g \sum_{\vec{p}_2 + \vec{p}_3 = \vec{p}_1} (p_2^2 - p_3^2) \psi_2(\vec{p}_2) \psi_3(\vec{p}_3) \tag{2.2}$$

and its cyclic permutations.  $\psi_\alpha(\vec{p})$  is the Fourier

component with momentum  $\vec{p}$  and  $\langle |\psi_\alpha^2(\vec{p})| \rangle = p^{-2}$  for all  $\alpha$ . Because of isotropy the decay rates associated with the different components are equal. This common rate which, in general, is a function of frequency, will be denoted by  $\gamma(k, \omega)$ . The corresponding Green's function is

$$g(k, \omega) = \frac{1}{-i\omega + \gamma(k, \omega)}. \quad (2.3)$$

The relaxation rate corresponding to the single loop of Fig. 1 (in the sense of a skeleton graph expansion) is given by

$$\begin{aligned} \gamma(k, \omega) = & \frac{g^2 k^2}{2\pi} \sum_{\vec{p}, \vec{p}'} \frac{(p^2 - p'^2)^2}{p^2 p'^2} \\ & \times \int g(p', \omega') g(p, \omega - \omega') d\omega', \end{aligned} \quad (2.4)$$

where  $\vec{p} + \vec{p}' = \vec{k}$ .

The above integral equation for  $\gamma(k, \omega)$  has a solution of the form

$$\gamma(k, z) = ak^x, \quad (2.5)$$

provided  $x = 1 + D/2$  and where  $z$  is the dimensionless imaginary frequency

$$z = -\frac{i\omega}{a(0)k^{1+D/2}}. \quad (2.6)$$

The convolution integral of Eq. (2.4) can be performed as explained in Ref. 7, leading to

$$\frac{\gamma(k, z)}{k^{1+D/2}} = \frac{I(z)}{a(1)}, \quad (2.7)$$

where

$$I(z) = \frac{1}{C_D} \int \frac{d^D p}{p^2 p'^2} \frac{(p^2 - p'^2)^2}{\frac{a(0)}{a(1)} z + p^{1+D/2} + p'^{1+D/2}}. \quad (2.8)$$

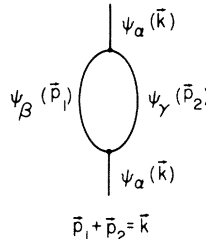


FIG. 1. Single-loop diagram for the order-parameter relaxation. Momentum conservation holds at the vertices.

This integral is logarithmically divergent at  $D = 6$ . To study the shape function to lowest order in  $\epsilon = 6 - D$ , we perform the following subtraction

$$\begin{aligned} I(z) &= I(0) + [I(z) - I(0)] \\ &= I(0) + F(z), \end{aligned} \quad (2.9)$$

where the subtracted integral  $F(z)$  can be evaluated at  $D = 6$  at this order of accuracy. Consequently,

$$\begin{aligned} F(z) = & \frac{1}{C_6} \int \frac{d^6 p (p^2 - p'^2)^2}{p^2 p'^2} \\ & \times \left[ \frac{1}{z + p^4 + p'^4} - \frac{1}{p^4 + p'^4} \right]. \end{aligned} \quad (2.10)$$

The leading  $I(0)$  in Eq. (2.10) needs to be calculated in the high momentum approximation only and yields  $I(0) = 2/3\epsilon$ . Equation (2.7) can then be written as

$$\gamma(k, z) = \gamma(k, 0) \left[ 1 + \frac{3\epsilon}{2} F(z) \right]. \quad (2.11)$$

Analytic evaluation of  $F(z)$  is not possible. After angular integration the remaining radial integration has to be performed numerically. The fluctuation spectrum results by taking the real part of Eq. (2.3). The results of the computation agree with Dohm's. The small  $-z$  behavior of  $F(z)$  can be computed analytically and yields

$$\begin{aligned} F(z) = & -\frac{z}{12} (6 + 6 \ln 2 - 3\pi) \\ & + \frac{z^2}{4} \left[ 1 - \frac{\pi}{4} \right] + \dots \end{aligned} \quad (2.12)$$

in agreement with Dohm. This expansion settles the question of the sign of the curvature at  $z = 0$ . It is elementary exercise to use Eqs. (2.3), (2.11), and (2.12) and show that to lowest order in  $\epsilon$  the curvature is downward for all  $\epsilon < 3.85$ . Thus at  $D = 3$  (i.e.,  $\epsilon = 3$ ), the curvature is certainly downward. The work of Nolan and Mazenko shows an upward curvature at the center. This can only be attributed to computational error. Before ending this section we wish to point out the true high frequency behavior of the self-energy and suggest a simple one-parameter approximation to  $\gamma(k, \omega)$  which we compare with the numerical computation in Fig. 2.

We turn now to the outer portions of the spectrum. Not being able to evaluate  $F(z)$  exactly we look for an interpolation formula. To this end, we

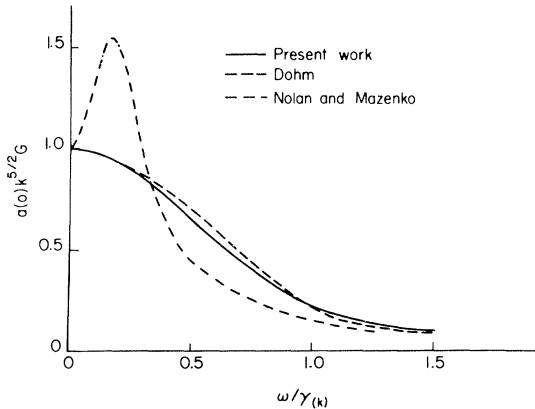


FIG. 2. Shape of the spectrum in the  $\epsilon$  expansion at the single-loop order. All the curves are normalized to equal area.

study the limit  $z \gg 1$ . Returning to Eq. (2.9), and being permitted to ignore the difference between  $a(0)$  and  $a(1)$  to lowest order in  $\epsilon$ , we find in this limit

$$\begin{aligned} I(z) &= \frac{4}{D} \int_0^\infty \frac{p^{D-3} dp}{z + 2p^{1+D/2}} \\ &= \frac{2}{D} \left[ \frac{2}{z} \right]^{\epsilon/(8-\epsilon)} \int_0^\infty \frac{x^{D-3} dx}{1+x^{1+D/2}} \\ &= \frac{4}{D(D+2)} \frac{\pi}{\sin[\pi\epsilon/(8-\epsilon)]} \left[ \frac{2}{z} \right]^{\epsilon/(8-\epsilon)}. \end{aligned} \quad (2.13)$$

We see that  $\gamma(z) \sim z^{-\epsilon/(8-\epsilon)}$  for  $z \gg 1$ . This is the correct high-frequency behavior of the self energy, as recognized by Dohm.<sup>2</sup> Subsequently, in a strict  $\epsilon$  expansion, the  $\epsilon$  in the denominator was dropped. Since in three dimensions  $\epsilon$  is large ( $\epsilon=3$ ) this can have an effect in the tail of the spectrum.

We now propose a one-parameter interpolation formula for  $F(z)$ . It is required to have the correct value both for the function and its first derivation at  $z=0$ , as well as the correct form for  $z \gg 1$ . These conditions are satisfied by

$$1 + \frac{3\epsilon}{2} F(z) = (1 + \beta z)^{-\epsilon/(8-\epsilon)}, \quad (2.14)$$

$$a_0^2 = a_0 a_1 \frac{a_0}{a_1} = \frac{2}{3\epsilon} \left\{ 1 + \epsilon \left[ \frac{1}{6} - \frac{1}{8} \left( \pi + \frac{1}{3} - 4 \ln 2 \right) - \frac{3}{2} F(1) \right] \right\}. \quad (3.3)$$

where  $F(z)$  is defined by Eq. (2.10). Since the integration cannot be done analytically, we have computed it numerically to find  $F(1) \simeq -0.02$ . Equation (3.3) is the  $O(\epsilon)$  result for the amplitude without the vertex correction.

The "vertex correction" diagram of Fig. 3(b) also contributes at this order. The contribution of this diagram to the zero-frequency relaxation rate is

where  $\beta$  is a numerical parameter. The derivative requires

$$\beta = \frac{(8-\epsilon)}{8} (6 + 6 \ln 2 - 3\pi), \quad (2.15)$$

which for  $\epsilon=3$  becomes

$$\beta = 0.46. \quad (2.16)$$

The coefficient of the high frequency tail comes out about 15% higher than that expected on the basis of Eq. (2.13). We thus expect Eq. (2.14) to be a good fit at very low frequencies, and then gradually deteriorate with a maximum error at 15% for  $z \gg 1$ . We note that at smaller values of  $\epsilon$ , the error is less and the interpolation even more satisfactory.

The fluctuation spectrum based on the self-energy of Eq. (2.14) is shown in Fig. 2. The corresponding spectra of Dohm<sup>2</sup> and of Nolan and Mazenko<sup>3</sup> are also exhibited for comparison. Note that the spectra have been normalized to equal area.

### III. THE UNIVERSAL AMPLITUDE

In this section we calculate the universal amplitude ratio<sup>10</sup> associated with the frequency scale at  $T_c$ . This is effectively the zero-frequency amplitude  $a_0 \equiv a(0)$  in Eq. (2.5). The  $O(\epsilon)$  contribution of self-energy insertions [Fig. 3(a)] in the single loop can be handled by a self-consistent treatment of Eqs. (2.7) and (2.8). It is seen from Eq. (2.11) that

$$a(z) = a_0 \left[ 1 + \frac{3\epsilon}{2} F(z) \right]. \quad (3.1)$$

From Eqs. (2.7) and (2.8) we obtain

$$\begin{aligned} a_0 a_1 &= I(0) \\ &= \frac{2}{3\epsilon} + \frac{1}{9} - \frac{1}{12} \left( \pi + \frac{1}{3} - 4 \ln 2 \right) + O(\epsilon). \end{aligned} \quad (3.2)$$

We note at this point that our result for  $I(0)$  differs from that of Dohm in the coefficient of  $\ln 2$ . Equations (3.1) and (3.2) yield

$$\gamma_v(k) = \frac{1}{C_D^2} \frac{2}{a_1(a_1 a_0)} \int \int \frac{d^D p_1 d^D p_2 (p_1^2 - p_1'^2)(p_2^2 - p_2'^2)}{p_2^2 p_1'^2 \left[ p_1^{1+D/2} + p_1'^{1+D/2} \right]} \times \frac{\left[ p_2^2 - |\vec{p}_1 - \vec{p}_2|^2 \right] \left[ p_1^2 - |\vec{p}_1 - \vec{p}_2|^2 \right]}{\left[ p_2^{1+D/2} + p_2'^{1+D/2} \right] \left[ p_1^{1+D/2} + p_1'^{1+D/2} + |\vec{p}_1 - \vec{p}_2|^{1+D/2} \right]}. \quad (3.4)$$

The overall factor of 2 arises from the two possible time orderings in Fig. 3(b). The frequency dependence of the intermediate lines can be neglected as the error involved is of  $O(\epsilon^2)$ . In the high momentum approximation  $p_1 \simeq p_1'$  and  $p_2 \simeq p_2'$ . Averaging over the direction of the external momentum  $\vec{k}$  leads then to

$$\langle (p_1^2 - p_1'^2)(p_2^2 - p_2'^2) \rangle \simeq \frac{4k^2}{D} \vec{p}_1 \cdot \vec{p}_2. \quad (3.5)$$

Using a momentum scale in which  $k = 1$ , and using  $a_1 a_0 \simeq 2/3\epsilon$ , we can write Eq. (3.4) in the form

$$v = \frac{3\epsilon}{D} \frac{1}{C_D} \int \frac{d^D p_1}{p_1^2 p_1^{1+D/2}} \frac{1}{C_D} \int \frac{d^D p_2}{p_2^2 p_2^{1+D/2}} (\vec{p}_1 \cdot \vec{p}_2) \frac{(p_2^2 - |\vec{p}_1 - \vec{p}_2|^2)(p_1^2 - |\vec{p}_1 - \vec{p}_2|^2)}{|p_1 - p_2|^2 (p_2^{1+D/2} + p_1^{1+D/2} + |p_1 - p_2|^{1+D/2})}, \quad (3.6)$$

where  $v$  denotes the contribution of the vertex correction to  $a_0 a_1$ . Using the scaled momentum  $p = p_2/p_1$  for the second integral, we can write Eq. (3.6) as

$$v = \frac{3\epsilon}{D} \frac{1}{C_D} \int \frac{d^D p_1}{p_1^2 p_1^{1+D/2}} \frac{1}{C_D} \int \frac{d^D p}{p^2 p^{1+D/2}} \frac{(\vec{1} \cdot \vec{p})(1 - |\vec{1} - \vec{p}|^2)(p^2 - |\vec{1} - \vec{p}|^2)}{|\vec{1} - \vec{p}|^2 (1 + p^{1+D/2} + |\vec{1} - \vec{p}|^{1+D/2})}. \quad (3.7)$$

The integration over  $p_1$  brings a factor of  $1/\epsilon$ . The remainder of integration may therefore be performed at  $D = 6$ . Hence,

$$v = \frac{1}{C_6} \int \frac{d^6 \vec{p} \vec{1} \cdot \vec{p} (1 - |\vec{1} - \vec{p}|^2)(p^2 - |\vec{1} - \vec{p}|^2)}{p^6 |\vec{1} - \vec{p}|^2 (1 + p^4 + |\vec{1} - \vec{p}|^4)}. \quad (3.8)$$

Equation (3.8) increases Eq. (3.2) to

$$a_0 a_1 = I(0) + v \quad (3.9)$$

so that Eq. (3.3) for  $a_0^2$  now becomes

$$a_0^2 = \frac{2}{3\epsilon} \left\{ 1 + \epsilon \left[ \frac{1}{6} - \frac{1}{8} \left( \pi + \frac{1}{3} - 4 \ln 2 \right) - \frac{3}{2} F(1) + \frac{3}{2} v \right] \right\} \quad (3.10)$$

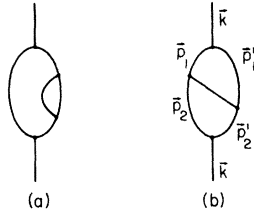


FIG. 3. Two-loop contributions to the relaxation rate. Figure 3(a) shows the self-energy insertion while Fig. 3(b) shows the vertex correction. Momentum conservation must hold at each vertex.

Thus the universal amplitude ratio to two-loop order is

$$a_0 = \left[ \frac{2}{3\epsilon} \right]^{1/2} \left\{ 1 + \frac{\epsilon}{2} \left[ \frac{1}{6} - \frac{1}{8} \left( \pi + \frac{1}{3} - 4 \ln 2 \right) - \frac{3}{2} F(1) + \frac{3}{2} v \right] \right\}. \quad (3.11)$$

In order to obtain a number for  $v$ , the six-dimensional integral of Eq. (3.8) has to be performed. Because of the quartic powers of  $p$  in the denominator, this integral cannot be performed analytically. Numerical evaluation, as seen in Appendix A, yields  $v \simeq 0.06$ . Thus, for  $\epsilon = 3$  the zero-frequency relaxation rate is

$$\gamma(k) = 0.61 k^{5/2}. \quad (3.12)$$

To compare with experimental results it is necessary to introduce the nonuniversal prefactor arising from the coupling constants. This can be represented by  $\sigma$ , where<sup>8</sup>

$$\sigma^2 = V k_B T_C (\mu_B g)^2 r_1^2 / 2 \pi^2 \hbar^2 \chi_0. \quad (3.13)$$

$V$  is the volume of the unit cell,  $r_1$  and  $\chi_0$  are defined by the Ornstein-Zernike susceptibility  $\chi = \chi_0 r_1^{-2} (k^2 + q^2)^{-1}$ , and the other symbols have the usual meaning. For EuO,  $\hbar \sigma a$  is 5.52 MeV  $\text{\AA}^{5/2}$ . Thus  $\hbar \gamma(k) = 3.37 k^{5/2}$  MeV  $\text{\AA}^{5/2}$ . The spec-

trum as given by Eq. (2.25) has the median frequency  $\Gamma=0.90\gamma$ . Thus our predicted width parameter for EuO for a two-loop calculation is

$$\hbar\Gamma = 3.03k^{5/2} \text{ MeV } \text{\AA}^{5/2}. \quad (3.14)$$

The observed amplitude<sup>8</sup> is about 30% higher.

For Co, we find the median frequency to be  $82 k^{5/2} \text{ MeV } \text{\AA}^{5/2}$  as compared to  $171 k^{5/2} \text{ MeV } \text{\AA}^{5/2}$  observed by Glinka *et al.*<sup>9</sup> The iron<sup>11</sup> and nickel<sup>12</sup> data were not analyzed in terms of non-Lorentzian spectra and hence cannot be compared with the theory. The  $\epsilon$  expansion is known<sup>13</sup> to give an underestimation of mode-coupling integrals owing to the neglect of the infrared divergence. The above discrepancy between theory and experiment is therefore not surprising.

#### IV. SUMMARY

We have determined the shape of the fluctuation spectrum of the isotropic ferromagnet to  $O(\epsilon)$  from the single-loop diagram. Our  $\epsilon$  expansion, which is independent of the renormalization group approach of Dohm<sup>2</sup> and of Nolan and Mazenko<sup>3</sup> would seem to settle the controversy regarding the existence of structure in the spectrum. Our analytic result for the curvature at the center agrees with

that of Dohm (apart from a minor detail) and thus confirms his conclusion that there is no peak in the spectrum at this order in  $\epsilon$ . We are in definite disagreement with the spin-wave-type peaked spectrum reported by Nolan and Mazenko and shown in Fig. 2.

We point out the existence of a very definite scaling form for the high-frequency tail of the spectrum. This condition on the high-frequency behavior has to be satisfied in the exponentiation of the  $\epsilon$  expansion results. The work of Dohm<sup>2</sup> and of Nolan and Mazenko<sup>3</sup> ignored this fact.

We have also carried out a two-loop calculation for the universal ratio associated with the amplitude of the zero-frequency relaxation rate. This leads to an expression for the width of the critical point spectrum, somewhat smaller than the experimental values, as expected for the  $\epsilon$  expansion. Being more qualitative, the  $\epsilon$ -expansion results for the shape can be expected to be more reliable.

#### ACKNOWLEDGMENTS

We wish to thank Dr. J. W. Lynn and Dr. C. J. Glinka for helpful conversations. This work was supported by NSF Grants DMR 79-00908 and 79-01172.

#### APPENDIX: VERTEX CORRECTIONS

In this appendix, we provide the details behind the calculation of the integral  $v$  defined in Eq. (3.8). Introducing the weight factor appropriate to the six-dimensional space and using a simple identity we can write

$$\begin{aligned} v &= \frac{4}{3\pi} \int_0^\infty \frac{p dp}{1+p^4} \int_0^\pi d\theta \sin^4\theta \cos\theta (2p \cos\theta - 1)(2 \cos\theta - p) \\ &\quad \times \left[ \frac{2}{1+p^2-2p \cos\theta} - \frac{(1+p^2-2p \cos\theta)}{1+p^2+p^4+2p^2 \cos^2\theta-2p(1+p^2)\cos\theta} \right] \\ &= v_1 - v_2, \end{aligned} \quad (A1)$$

where

$$v_1 = \frac{8}{3\pi} \int_0^\infty \frac{p dp}{1+p^4} \int_0^\pi d\theta \sin^4\theta \cos\theta \frac{[p(1+4 \cos^2\theta)-2(1+p^2)\cos\theta]}{1+p^2-2p \cos\theta} \quad (A2)$$

and

$$v_2 = \frac{4}{3\pi} \int_0^\infty \frac{p dp}{1+p^4} \int_0^\pi d\theta \sin^4\theta \cos\theta \frac{(1+p^2-2p \cos\theta)[p-2(1+p^2)\cos\theta+4p \cos^2\theta]}{1+p^2+p^4-2p(1+p^2)\cos\theta+2p^2 \cos^2\theta}. \quad (A3)$$

$v_1$  can be evaluated exactly by noting that

$$\sin^4\theta(1+4\cos^2\theta) = \frac{1}{8}(5-5\cos 2\theta - \cos 4\theta + \cos 6\theta), \quad (\text{A4})$$

$$\sin^4\theta \cos^2\theta = \frac{1}{32}(2 - \cos 2\theta - 2\cos 4\theta + \cos 6\theta), \quad (\text{A5})$$

$$\int_0^\pi \frac{\cos n\theta d\theta}{1+p^2-2p\cos\theta} = \begin{cases} \frac{\pi p^n}{1-p^2}, & p^2 < 1 \\ \frac{\pi p^{-n}}{p^2-1}, & p^2 > 1 \end{cases} \quad (\text{A6})$$

and

$$\int_0^\pi \frac{\cos n\theta \cos\theta d\theta}{1+p^2-2p\cos\theta} = \begin{cases} \frac{\pi}{2} \frac{1+p^2}{1-p^2} p^{n-1}, & p^2 < 1 \\ \frac{\pi}{2p^{n+1}} \frac{p^2+1}{p^2-1}, & p^2 > 1. \end{cases} \quad (\text{A7})$$

Carrying out the elementary radial integrations we

find

$$v_1 = \frac{1}{12} \left[ \ln 2 - \frac{\pi}{2} \right]. \quad (\text{A8})$$

The integral  $v_2$  cannot be done analytically. We see from Eq. (A3) that for  $p \rightarrow 0$ , the angular integration yields  $-\pi/8$ . For  $p \rightarrow \infty$  too, the angular integration yields  $-\pi/8$ . Numerical evaluation of the integral for various values of  $p$  shows it to be remarkably constant and approximately equal to  $-0.40$  or  $-\frac{2}{5}$ . Thus,

$$v_2 \simeq -\frac{4}{3\pi} \times \frac{2}{5} \times \int_0^\infty \frac{p dp}{1+p^4} = -\frac{4 \times 2 \times \pi}{3 \times 5 \times \pi \times 4} = -\frac{2}{15}, \quad (\text{A9})$$

leading to

$$v = v_1 - v_2 = \frac{1}{12} \left( \ln 2 - \frac{\pi}{2} + \frac{8}{5} \right) \simeq 0.06, \quad (\text{A10})$$

the result quoted in the text.

\*Part of the Ph. D. thesis of J. K. B., University of Maryland, 1979 (unpublished).

<sup>1</sup>S. Ma and G. Mazenko, Phys. Rev. B **11**, 4077 (1970).

<sup>2</sup>V. Dohm, Solid State Commun. **20**, 659 (1976).

<sup>3</sup>M. Nolan and G. Mazenko, Phys. Rev. B **15**, 4077 (1977).

<sup>4</sup>F. Wegner Z. Phys. **216**, 433 (1968). [See also E. K. Riedel, J. Appl. Phys. **42**, 1383 (1971) and J. Hubbard, J. Phys. C **4**, 53 (1971).]

<sup>5</sup>R. Freedman and G. Mazenko, Phys. Rev. B **13**, 4967 (1976).

<sup>6</sup>R. A. Ferrell, V. Dohm, and J. K. Bhattacharjee, Phys. Rev. Lett. **41**, 1818 (1978).

<sup>7</sup>R. A. Ferrell and J. K. Bhattacharjee, J. Low Temp.

Phys. **36**, 165 (1979).

<sup>8</sup>O. W. Dietrich, J. Als-Nielsen, and L. Passell, Phys. Rev. B **14**, 4923 (1976).

<sup>9</sup>C. J. Glinka, V. J. Minkiewicz, and L. Passell, Phys. Rev. B **16**, 4084 (1977).

<sup>10</sup>P. C. Hohenberg and B. I. Halperin, Rev. Mod. Phys. **49**, 435 (1977).

<sup>11</sup>M. F. Collins, R. Nathans, L. Passell, and G. Shirane, Phys. Rev. **179**, 417 (1969).

<sup>12</sup>V. J. Minkiewicz, M. F. Collins, R. Nathans, and G. Shirane, Phys. Rev. **182**, 624 (1969).

<sup>13</sup>J. K. Bhattacharjee and R. A. Ferrell, J. Low Temp. Phys. **36**, 165 (1979); J. Math Phys. **21**, 534 (1980).